International Journal of Pharmaceutics 400 (2010) 165–175

Contents lists available at ScienceDirect

International Journal of Pharmaceutics

journal homepage: www.elsevier.com/locate/ijpharm

Pharmaceutical Nanotechnology

Amphiphilic PHA–mPEG copolymeric nanocontainers for drug delivery: Preparation, characterization and *in vitro* evaluation

Mohsin Shah [a], Muhammad Imran Naseer [b], Mun Hwan Choi [a], Myeong Ok Kim [b], Sung Chul Yoon [a,*]

[a] *Nano-Biomaterials Science Laboratory, Division of Applied Life Sciences (BK21), Graduate School and Environmental Biotechnology National Core Research Center, Gyeongsang National University, Jinju 660-701, Republic of Korea*
[b] *Neurobiology Laboratory, Division of Life Science, College of Natural Sciences and Division of Applied Life Sciences (BK21), Gyeongsang National University, Jinju 660-701, Republic of Korea*

ARTICLE INFO

Article history:
Received 9 April 2010
Received in revised form 4 August 2010
Accepted 9 August 2010
Available online 14 August 2010

Keywords:
PHA–mPEG
Biodegradable polymers
Amphiphilic nanoparticles
Biocompatibility
Drug release

ABSTRACT

Amphiphilic biodegradable core–shell nanoparticles were prepared by emulsification–solvent evaporation technique from diblock copolymers which were synthesized by chemical coupling of poly(3-hydroxybutyrate-*co*-3-hydroxyvalerate) P(3HB-*co*-3HV) or poly(3-hydroxybutyrate-*co*-4-hydroxybutyrate) P(3HB-*co*-4HB) to monomethoxy poly(ethylene glycol) (mPEG) through transesterification reaction. The nanoparticles were found to be assembled in aqueous solution into an outer hydrophilic shell of mPEG connected to the interior hydrophobic polyhydroxyalkanoate (PHA) copolymer core, which was identified by a comparative analysis of enzymatic degradation of the mPEG-coupled and non-coupled PHA nanoparticles. Morphological examination under atomic force microscope showed the formation of smooth spherically shaped nanoparticles. The average particle sizes and zeta potentials of amphiphilic nanoparticles were in the range of 112–162 nm and −18 to −27 mV, respectively. A hydrophobic drug thymoquinone was encapsulated in the nanoparticles and its release kinetics was studied. The *in vitro* cytotoxicity evaluation of the nanoparticles on prenatal rat neuronal hippocampal and fibroblast cells revealed that biocompatibility of the amphiphilic nanoparticles was generally independent of the ratio of comonomer units in the PHA block. In conclusion, the amphiphilic nanoparticles contained the hydrophobic PHA segments buried in the core and could thus be used as safe carriers for the controlled release of variety of hydrophobic drugs.

1. Introduction

Over the past few decades, there has been considerable progress in developing biodegradable nanoparticles as effective drug delivery devices (Soppimath et al., 2001). Different types of biodegradable polymers both synthetic and natural have been utilized in the preparation of nanoparticles (Moghimi et al., 2001; Hans and Lowman, 2002). Nanoparticles are submicron-sized polymeric colloidal particles with a size range from 1 to 1000 nm and drugs may be encapsulated, adsorbed or dispersed in them (Soppimath et al., 2001; Panyam and Labhasetwar, 2003; Letchford and Burt, 2007). Recently, biodegradable polymeric nanoparticles as drug carriers have attracted great research interest because of their biocompatibility, biodegradability and sustained release of drugs (Panyam and Labhasetwar, 2003). Polyhydroxyalkanoates (PHA) are biodegradable thermoplastic polymers produced by microorganisms during unbalanced growth condition as inclusion bodies (Anderson and Dawes, 1990; Lenz and Marchessault, 2005). Different types of PHA homopolymers and copolymers produced by microorganisms have been suggested to be utilizable as tissue engineering materials and controlled release drug vectors (Khang et al., 2001; Köse et al., 2003; Timbart et al., 2004; Yao et al., 2008). Microparticles prepared from either poly(3-hydroxybutyrate-*co*-3-hydroxyvalerate) (PHBV) or blends of PHBV and polycaprolactone were used for the sustained release of drugs (Khang et al., 2001; Lionzo et al., 2007). Similarly, wafers produced from PHBV were also utilized for the release of antibiotics (Khang et al., 2000). Nanoparticles prepared from poly(3-hydroxybutyrate) (PHB) are getting much attention because it provides a safe, nontoxic and biodegradable surface for coating with other materials (Pötter and Steinbüchel, 2005). Apart from that, according to ISO 10993, toxicity experiment on PHB indicated that the substance is safe to be used as nanoparticles in animals (Pötter and Steinbüchel, 2005). However, direct administration of unmodified microbial polyesters as therapeutic agents were found to induce inflammatory responses in animal tissues (Qu et al., 2006).

The surface modification of a polymer with nontoxic and blood compatible material is essential in order to avoid recognition by

* Corresponding author. Tel.: +82 55 751 5942; fax: +82 55 753 0765.
E-mail address: scyoon@gnu.ac.kr (S.C. Yoon).

0378-5173/$ – see front matter © 2010 Elsevier B.V. All rights reserved.
doi:10.1016/j.ijpharm.2010.08.008

macrophages, to prolong blood circulation time and sustained release of the encapsulated drugs (Mosqueira et al., 2001; Duan et al., 2006). Poly(ethylene glycol) (PEG) is widely used as hydrophilic nontoxic segment in combination with hydrophobic biodegradable aliphatic polyesters (Gref et al., 1994; Avgoustakis et al., 2003; Kumar and Homme, 2008; Basu et al., 2009). Incorporation of a hydrophilic mPEG group on the surface of nanoparticles was found to show resistance against opsonization and phagocytosis and showed prolonged residence time in blood compared to the nanoparticles prepared without mPEG (Gref et al., 1994; Avgoustakis et al., 2003; Basu et al., 2009). Surface modification of a polymer with this nontoxic material reduces the risk of side effects developed by the unmodified polymers (Kumar and Homme, 2008). Moreover, PEG has been approved by the Food and Drug Administration for human use and the mPEG released from the degradation of polyester–mPEG block polymers can be easily removed from the body via kidneys (Fishburn, 2008; Tang and Sing, 2009).

Low molecular weight biodegradable block copolymers in the form of amphiphilic nanoparticles were suggested to be used as sustained release of variety of hydrophobic drugs (Chen et al., 2006; Tang and Sing, 2009). The use of amphiphilic block copolymers is advantageous because they possess unique physicochemical characteristics such as self-assembly and thermodynamic stability in aqueous solution (Gaucher et al., 2005). In the amphiphilic structure of polymeric micelles, hydrophobic drug molecules are solubilized within the hydrophobic cores, whereas the shell maintains a hydration barrier that protects the integrity of each micelle (Prabaharan et al., 2009). Encapsulation of drug in the polymeric nanoparticles can deliver effective dose of the pharmacologically active substance to its specific site, particularly to the tumor for the sustained period of time that could avoid the side effects associated with multiple dosing of the drug (Duncan, 2006). Polymeric nanoparticles can easily permeabilize the tumor tissues due to the defective and leaky structure of tumor vessels and impaired lymphatic system taking advantage of the enhanced permeability and retention (EPR) effect (Maeda et al., 2000; Iyer et al., 2006; Bisht and Maitra, 2009).

Most of the matrix studies to date focused on the utilization of PHA copolymers at the level of micron sized particles using high molecular weight unmodified PHA copolymers as a component or a blend form mixed with other polyester (Sendil et al., 1999; Lionzo et al., 2007). However, compared to nanoparticles, the microparticles are bigger and difficult to cross cellular membranes of the body (Panyam and Labhasetwar, 2003). A decreased rate of clearance and extended circulation time have also been observed in the nanoparticles with smaller diameter as compared to those with larger diameter (Moghimi et al., 1993). Therefore, nanoparticles preparation with smaller diameter from the low molecular weight PHA–mPEG diblock copolymers may enhance the therapeutic application of these materials for drug delivery.

In this study, PHA–mPEG diblock copolymers with different composition of PHA copolymers were synthesized. These copolymers were then assembled into core–shell nanoparticles using emulsification–solvent evaporation method. To the best of our knowledge this is the first report which describes the synthesis of nanoparticles utilizing PHA copolymers in combination with mPEG as nontoxic biocompatible material. The formed nanoparticles were characterized in terms of morphology, size, surface charge and core–shell assembly. To assess the suitability of the nanoparticles as delivery vehicles for hydrophobic drugs, thymoquinone (TQ) was employed as a model hydrophobic drug in the nanoparticles and studied its release kinetics *in vitro*. The biocompatibility of the nanoparticles was evaluated *in vitro* using prenatal rat neuronal hippocampal cells and NIH/3T3 fibroblast cell line.

2. Materials and methods

2.1. Materials

The copolymers P(3HB-*co*-12 mol% 3HV) and P(3HB-*co*-33 mol% 3HV) were produced by *Hydrogenophaga pseudoflava* 33668 in PHA synthesis mineral medium containing 10 g/L glucose and 0.4 and 1.5 mL/L γ-valerolactone, respectively, and cultivated at 35 °C for 96 h. The copolymers P(3HB-*co*-6 mol% 4HB) and P(3HB-*co*-20 mol% 4HB) were produced by cultivating *Ralstonia eutropha* H16 in PHA synthesis mineral medium containing 10 g/L fructose and 1 and 4 mL/L ε-caprolactone, respectively, at 30 °C for 96 h. Monomethoxy poly(ethylene glycol), mPEG [number average molecular weight (M_n) = 2000], bis(2-ethylhexanoate) tin catalyst, sodium deoxycholate, dichloromethane (DCM), and TQ were purchased from Sigma–Aldrich Korea Ltd. All other chemicals used were of analytical grades. Polyesters were extracted from an appropriate amount of cells, which had been dried overnight at 50 °C under a vacuum. Extraction was performed with hot chloroform in a Pyrex Soxhlet apparatus for 6 h. The concentrated solvent extract was precipitated in rapidly stirred cold methanol.

2.2. Synthesis of diblock copolymers

The synthesis of PHA–mPEG diblock copolymers was carried out by transesterification method in the melt as previously described (Ravenelle and Marchessault, 2002, 2003). Briefly, a 25 mL round bottom flask was loaded with weight ratio of 1:1 of the PHA copolymer and mPEG fitted with magnetic stirrer. The reaction was carried out in a preheated oil bath at 190 °C, under vacuum. Almost 70 mg of the bis(2-ethylhexanoate) tin catalyst was added into the flask through a rubber septum using a syringe under the flow of nitrogen. The reaction was done for 20–30 min with continuous stirring. After completion, the flask was removed and cooled in ice or at room temperature yielding a waxy product. The PHA–mPEG diblock copolymer obtained was dissolved in 5 mL chloroform and then poured dropwise into 100 mL distilled water forming an emulsion. The emulsion was stirred vigorously with a magnetic stirrer to evaporate the organic solvent. A colloidal suspension was formed which was purified by dialyzing against distilled water using 12,000–14,000 Da molecular weight cutoff membrane for a week. The resulting purified diblock copolymer was then lyophilized to obtain light whitish powder (yield 70–80%).

2.3. Characterization of diblock copolymers

Molecular weights and polydispersities of the diblock copolymers were determined by gel permeation chromatography (GPC) measurements at 30 °C using an Agilent 1100 series Gel Permeation Chromatography system (Agilent, Santa Clara, CA), consisting of a series of three PLgel columns (10^5, 10^3, and 10^2), an Agilent G1310A Isocratic pump, an Agilent 1047A RI detector, an Agilent G1316A column compartment, and an Agilent G1311A vacuum degasser. Chloroform was used as eluent at a flow rate of 1.0 mL/min. Polystyrene standards (Polymer Laboratories, Amherst, MA), with low polydispersity was used for system calibration.

The molecular structures of diblock copolymers were obtained by ^{1}H NMR with Bruker-DRX-500 MHz spectrometer (Choi and Yoon, 1994; Choi et al., 1999). The spectra of the samples were recorded at room temperature in $CDCl_3$. The integration of the split spectral signals was performed with standard software.

Thermal transitions of the diblock copolymers were measured under nitrogen purging by using a differential scanning calorimeter (DSC) Q200 (TA Instruments, New Castle, DE), equipped with a data station. The heating rate was 10 °C/min. The scanning range was between −50 and 190 °C.

Quantitative determination of the comonomer composition of the polyesters was determined by analyzing the methyl esters, recovered from a sulfuric acid/methanol treatment of the polyesters, using a Hewlett Packard HP5890 Series II gas chromatograph equipped with a HP-1 capillary column and a flame ionization detector (Choi and Yoon, 1994).

2.4. Preparation of nanoparticles

Drug loaded amphiphilic nanoparticles were prepared from the diblock copolymers by way of a slightly modified emulsification–solvent evaporation technique, as described previously (Budhian et al., 2007). Briefly, the diblock copolymer (50 mg) and TQ (5 mg) were dissolved in 3 mL of DCM under continuous stirring. This mixture was added to a 12 mM sodium deoxycholate solution (50 mL) and the mixture was probe sonicated at 20% power for 10 min using a microtip probe sonicator D-12207 (Bandelin Electronics, Germany). The emulsion formed was then gently stirred in a fume hood at room temperature until complete evaporation of the organic phase was achieved. The nanoparticles were purified by centrifugation at 12,000 rpm for 10 min and then washed with fresh water two times to remove the excessive emulsifier and unentrapped free drug. After centrifugation, the amount of TQ in the supernatant was assayed by spectrophotometer (Hewlett Packard UV 8452A) at a wavelength of 450 nm. The drug encapsulation efficiency of PHA–mPEG nanoparticles was carried out as described previously (Ravindran et al., 2010). Drug free nanoparticles were prepared by the same method. Four different types of drug loaded and unloaded nanoparticles (P(3HB-*co*-12 mol% 3HV)–mPEG, P(3HB-*co*-33 mol% 3HV)–mPEG, P(3HB-*co*-6 mol% 4HB)–mPEG and P(3HB-*co*-20 mol% 4HB)–mPEG) were prepared and used in this study.

2.5. Characterization of nanoparticles

Morphology of nanoparticles was analyzed by atomic force microscope (AFM) (Park Systems, PSIA XE-100). The nanoparticles suspension was dropped onto the freshly cleaved mica surface with the help of a pipette and allowed to dry at 30 °C in incubator. The images were obtained using non-contact mode. The cantilever used for scanning was 125 μm × 30 μm with a nominal force constant of 42 N/m. The analysis of images was performed with XEI 1.7.1 software.

Particle sizes and size distributions were determined by the light-scattering method (DLS-8000; Otsuka Electronics Co., Osaka, Japan). For particle size analysis, approximately 10 mL of the nanoparticles suspension was prepared in water and optically analyzed at a scattering angle of 90°. The mean particle size of each sample was determined in triplicate and the average values were calculated. The surface charge of the nanoparticles was measured in phosphate buffered saline (PBS, pH 7.4) and was characterized in terms of zeta potential using electrophoretic light-scattering spectrophotometer (ELS-8000; Otsuka Electronics Co., Osaka, Japan) at a scattering angle of 20°.

The core–shell assembly of nanoparticles in aqueous solution was spectrophotometrically characterized by following enzymatic degradation of P(3HB-*co*-12 mol% 3HV)–mPEG and P(3HB-*co*-20 mol% 4HB)–mPEG diblock copolymers nanoparticles and compared with the particles prepared from P(3HB-*co*-12 mol% 3HV) and P(3HB-*co*-20 mol% 4HB) copolymers. *Ralstonia pickettii* T1 (obtained from Prof. Saito, Kanagawa University, Japan) was used as a source strain of PHB depolymerase. A stable suspension (the initial absorbance 3.0 ± 0.03 at 660 nm) of the copolymer particles and mPEG capped nanoparticles was prepared with ultra-sonication, suspended in 50 mM Tris–HCl containing 1 mM $MgCl_2$ (pH 8.0). The degradation reaction in a shaker bath at 37 °C was initiated by the addition of 0.2 μg/mL of purified enzyme. The decrease in turbidity was measured at 660 nm with a spectrophotometer (Hewlett Packard UV 8452A).

2.6. In vitro drug release studies

The measurement of TQ release from the drug loaded nanoparticles *in vitro* was carried out in a glass apparatus containing 50 mL of PBS (pH 7.4) at 37 °C as described previously (Prabaharan et al., 2009). In Brief, 50 mg of the drug loaded nanoparticles was dispersed in 5 mL of PBS and placed into a cellulose membrane dialysis tube (molecular weight cutoff = 3000–3500 Da). The dialysis tube was then immersed in the release medium (50 mL) and incubated in a shaker bath (100 rpm) at 37 °C. Aliquots of 1 mL were periodically withdrawn from the solution. The volume of the solution was held constant by adding 1 mL of fresh buffer solution after each sampling to ensure sink condition. The amount of TQ released in the medium was analyzed spectrometrically at 450 nm. The percent release of the TQ was then plotted as a function of dialysis time. For the control experiment, 5 mg of free TQ was dissolved in DCM and poured into 5 mL of PBS and sonicated. The organic solvent was evaporated by stirring and most TQ remained dissolved in the medium with little amount of suspended TQ particles. All experiments were repeated in triplicate.

2.7. In vitro biocompatibility

2.7.1. Cell culture

The effect of toxicity of the nanoparticles was evaluated using two types of cells; prenatal rat neuronal hippocampal cells and NIH/3T3 fibroblast cell line. For the isolation of neuronal cells, female (n = 7) Sprague–Dawley rats (250 g, Gyeongsang National University, Neurobiology Laboratory, Jinju, South Korea) were housed in a temperature-controlled environment with lights from 06:00–20:00 h with food ad libitum. Pregnant rat after (gestational days) GD 17.5 (time of pregnancy was considered from the day of insemination equals to GD 0.5) was killed by decapitation and fetus were removed. Primary cell cultures were prepared from the hippocampal neurons of prenatal rat. Pooled hippocampal tissues were treated with 0.25% trypsin–EDTA for 20 min and dissociated by mechanical trituration in ice-cold calcium and magnesium-free Hank's balanced salt solution (pH 7.4). After pelleting by centrifugation, cells were plated (1×10^6 cells/mL) in cell culture plates pre-coated with polylysine (0.02 g/L) and chamber slides. The cells were maintained in Dulbecco's modified Eagle's medium (DMEM) supplemented with 10% heat-inactivated fetal bovine serum, 1 mM pyruvate, 4.2 mM sodium bicarbonate, 20 mM HEPES, 0.3 g/L bovine serum albumin, 50 U/mL penicillin, and 50 mg/L streptomycin. The NIH/3T3 fibroblast cell line (KCLB 21658) was obtained from the Korean Cell Line Bank (KCLB, Seoul Korea) and were cultured in DMEM with 10% FBS and incubated for 48 h. A humidified atmosphere at 37 °C with 5% CO_2 and 95% air was used for maintenance of cell culture.

2.7.2. MTT assay

The *in vitro* effect of nanoparticles on toxicity of cells was investigated by the 3-(4,5-dimethylthiazol-2-yl)-2,5-diphenyltetrazolium bromide (MTT) assay. The cells were seeded in 96-well plates and incubated at 37 °C. The nanoparticles dispersions (100–500 μg/mL) were added to the cells at desired concentrations and incubated for 24 h. Cells with culture medium but with no added nanoparticles were used as positive control. The cells were incubated at 37 °C for 24 h in a humidified 5% CO_2 incubator. After incubation cell viability was determined by adding MTT (5 mg/mL in PBS pH 7.4) to each well and incubated for 4 h at 37 °C. To achieve solubilization of formazan crystal formed in viable

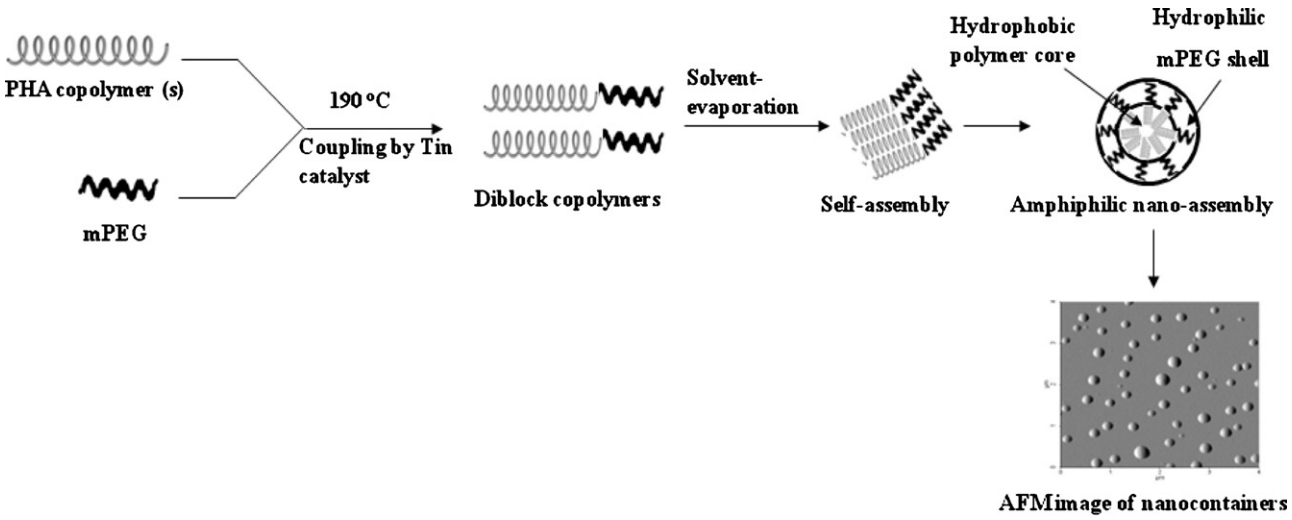

Fig. 1. A model for the formation of amphiphilic copolymeric nanocontainers from PHA–mPEG diblock copolymers.

cells, dimethylsulfoxide was added to each well. The absorbance of viable cells was measured at 570 nm using a microplate reader (Anthos 2020, Anthos Labtech Instruments, Wals., Austria). The cell viability (%) relative to control wells containing cell culture without nanoparticles was calculated by $[A]_{test}/[A]_{control} \times 100$.

2.7.3. Fluoro-Jade-B (FJB) staining

Fluoro-Jade-B (FJB) staining was performed as previously described (Johnson, 1995; Naseer et al., 2010). Briefly, primary hippocampal neuronal cell cultures were grown *in vitro* on polylysine-coated chamber slides. Cells were treated with normal medium as control and with nanoparticles dispersion (100–500 μg/mL) and were incubated for 24 h at 37 °C. Chamber slides were washed with PBS three times for 5 min each and fixed for 5 min with 4% paraformaldehyde in PBS and stored at −70 °C. Next day the slides were air dried for 3 h and then transferred in 0.06% potassium permanganate solution for 10 min. After rinsing in water, slides were immersed in a solution of 0.1% acetic acid and 0.0004% FJB (Calbiochem, San Diego, CA, USA) for 20 min. Slides were washed 3 times with distilled water and allowed to dry at 55 °C for 10 min. Glass cover slips were mounted on glass slides with mounting medium. For images FITC filter was used in confocal microscope (Fluoview Olympus, Japan).

2.8. Statistical analysis

All results were expressed as mean ± standard deviation of experiment performed in triplicates. Statistical differences were evaluated using a one-way analysis of variance (ANOVA) with student's *t*-test. Differences were considered to be statistically significant at a level of $P < 0.05$.

3. Results and discussion

3.1. Synthesis and characterization of PHA–mPEG diblock copolymers

The transesterification reaction was carried out in the melt at 190 °C for 20–30 min (Scheme 1). In this reaction high molecular weight PHA copolymers were first depolymerized into low molecular weight macromolecules (Naguyen et al., 2002). The low molecular weight macromolecules formed reacted with mPEG in the presence of bis(2-ethylhexanoate) tin as transesterification catalyst giving block copolymers (Ravenelle and Marchessault, 2002). A model for the synthesis of diblock copolymers and their subsequent self-assembly into nanoparticles is also depicted in Fig. 1.

GPC analysis was carried out in order to determine the molecular weights and molecular weight distributions of diblock copolymers. GPC chromatograms of the purified diblock copolymers and precursor mPEG are shown in Fig. 2. The GPC chromatograms of the diblock copolymers exhibited a rather broader unimodal peak shifted towards higher molecular weights as compared to that of mPEG prepolymer (Ravenelle and Marchessault, 2002). The appearance of such unimodal peak indicated that no significant amount of unreacted free precursor prepolymers remained in the purified product. Table 1 lists the number average molecular weights (M_n), weight average molecular weights (M_w) and polydispersities (M_w/M_n) of the diblock copolymers.

The chemical coupling between the carboxyl terminal of PHA and hydroxyl terminal of mPEG in diblock copolymers (Ravenelle and Marchessault, 2002) was confirmed by ^{1}H NMR spectroscopy. The chemical coupling for P(3HB-*co*-12 mol% 3HV)–mPEG and P(3HB-*co*-6 mol% 4HB)–mPEG is shown in Fig. 3A and B, respectively. In Fig. 3A peaks (a)–(j) are associated with P(3HB-*co*-12 mol% 3HV) and peaks (k), (l) and (m) with mPEG. The peak (k) at 4.18 ppm must be ascribed to the methylene-unit (located at the hydroxyl terminal of mPEG chain) involved in the coupling between the PHA and mPEG chain. Similar to PHB–mPEG, P(3HB-*co*-12 mol%

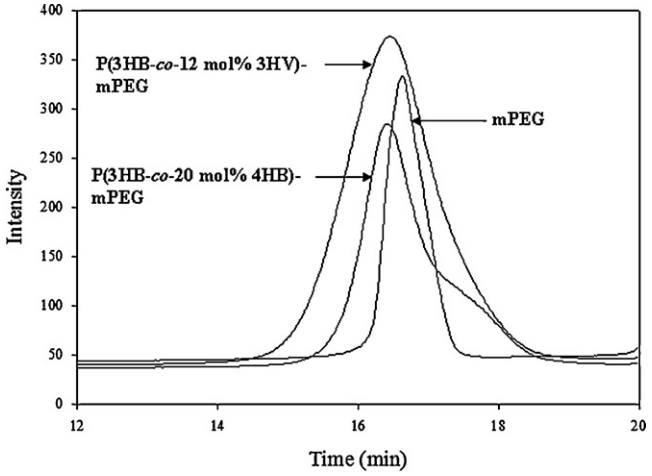

Fig. 2. GPC chromatograms of the PHA–mPEG diblock copolymers and free mPEG.

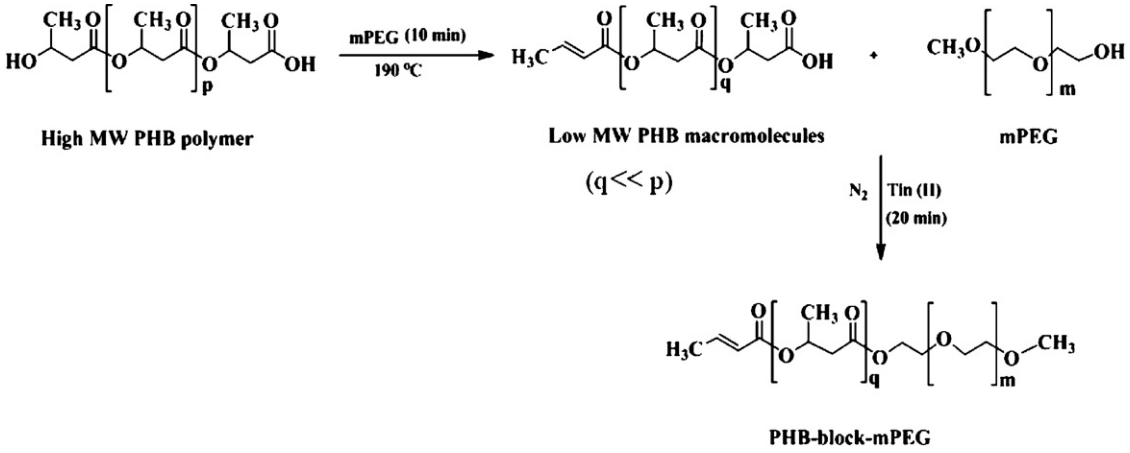

Scheme 1. The synthetic scheme for the formation of PHA–mPEG diblock copolymers using bis(2-ethylhexanoate) tin catalyst following the Ravenelle and Marchessault procedure (Ravenelle and Marchessault, 2002).

3HV)–mPEG also exhibited two minor absorption peaks at 6.96 and 5.75 ppm (c and d, respectively) associated with the olefinic end group resulting from thermal dehydration of the hydroxyl terminal group (Ravenelle and Marchessault, 2002). A similar coupling was observed for P(3HB-*co*-6 mol% 4HB)–mPEG diblock copolymer (Fig. 3B).

Thermal transitions of the diblock copolymers were determined by DSC analysis. All scans were run from −50 to 190 °C, except for mPEG which ranged from 35 to 100 °C. Table 1 lists the melting temperatures (T_m) of the diblock copolymers. The T_m values of mPEG block were observed in the range of 43.1–49.3 °C while for PHA copolymer block from 129.7 to 140.5 °C.

3.2. Preparation and characterization of nanoparticles

Amphiphilic core–shell biodegradable nanoparticles were prepared from the PHA–mPEG diblock copolymers by emulsification–solvent evaporation technique (Fig. 1). In order to investigate the morphology of the prepared nanoparticles, AFM observations were conducted. Fig. 4A and B shows typical non-contact AFM images of the P(3HB-*co*-33 mol% 3HV)–mPEG and P(3HB-*co*-20 mol% 4HB)–mPEG nanoparticles, respectively. The AFM images show that the nanoparticles formed as a result of solvent evaporation were discrete spherically shaped and smooth in surface morphology, with an average diameter of less than 200 nm. But the P(3HB-*co*-33 mol% 3HV)–mPEG and P(3HB-*co*-20 mol% 4HB)–mPEG nanoparticles sample exhibited some nonuniformly distributed particles in the AFM image (Fig. 4A and B). However, when the level of 3HV or 4HB was decreased like P(3HB-*co*-12 mol% 3HV)–mPEG and P(3HB-*co*-6 mol% 4HB)–mPEG relatively uniform distributed particles were observed (data not shown). The larger particles observed might be due to some aggregation of the nanoparticles especially the nanoparticles formed from high mole ratios of 3HV or 4HB comonomer unit in the composition. A similar comonomer-ratio dependent behavior was also found for PLGA copolymer nanoparticles (Budhian et al., 2007). The size distributions of the nanoparticles determined by DLS (Fig. 4C and D) are in agreement with the result obtained from AFM.

The particle sizes, polydispersities and surface charges of the nanoparticles are listed in Table 2. The average sizes ranged from 100 to 200 nm and the zeta potential values from −18 to −27 mV. All the nanoparticles preparation exhibited negative zeta potential values. A more negative zeta potential of the nanoparticles suggested more dispersion stability of the nanoparticles in the medium (Jeong et al., 2009). Thus, the PHA–mPEG nanoparticles form a stable colloidal suspension in aqueous medium. Moreover, the amphiphilic nature of the nanoparticles causes to repel them to stabilize each other and to prevent aggregation.

To understand the core–shell topography of the PHA–mPEG nanoparticles, a comparative enzymatic degradation was carried out against PHA–mPEG and PHA particles in the presence of (0.2 μg/mL) PHB depolymerase from *R. pickettii* T1. *R. pickettii* T1 PHB depolymerase is known to scissor the second or third ester linkage of the polyester chain and behave as an endo-degrading enzyme for PHB substrates (Shirakura et al., 1986). However, the ability to degrade single crystals from the edges and ends of crystals indicated that this enzyme has exo-degrading behavior in addition to the endo-degrading mode of action (Iwata et al., 1999). The degradation reaction was followed by measuring turbidity of the reaction solution at 660 nm using purified enzyme from *R. pickettii T1*. Fig. 5 shows the degradation profiles of two mPEGylated nanoparticles P(3HB-*co*-12 mol% 3HV)–mPEG and P(3HB-*co*-20 mol% 4HB)–mPEG and two non-mPEG counterpart particles P(3HB-*co*-12 mol% 3HV) and P(3HB-*co*-20 mol% 4HB). The PEGylated sample was degraded very slowly compared to the counterpart non-mPEG control sample (Fig. 5). A plausible explanation for the slower degradation rate of all mPEGylated systems was due to the coverage of the enzymatically inactive mPEG segment on the surface of enzymatically active PHA copolymer core. A similar

Table 1
Molecular weights and thermal properties of PHA–mPEG diblock copolymers.

Diblock copolymer	M_w[a]	M_n[a]	PI (M_w/M_n[a])	Yield[b] (%)	T_m[c] (°C) PHA block	T_m[c] (°C) mPEG block
P(3HB-*co*-12 mol% 3HV)–mPEG	8980	6200	1.44	75	140.5	49.1
P(3HB-*co*-33 mol% 3HV)–mPEG	4980	2650	1.87	78	133.6	49.3
P(3HB-*co*-6 mol% 4HB)–mPEG	5310	3580	1.48	76	133.7	43.1
P(3HB-*co*-20 mol% 4HB)–mPEG	7330	5230	1.40	73	129.7	47.8

[a] Determined by GPC.
[b] Ratio of the weight of product formed to the weight of added mPEG and copolymer at the start.
[c] Melting temperatures of the PHA–mPEG diblock copolymers determined by DSC.

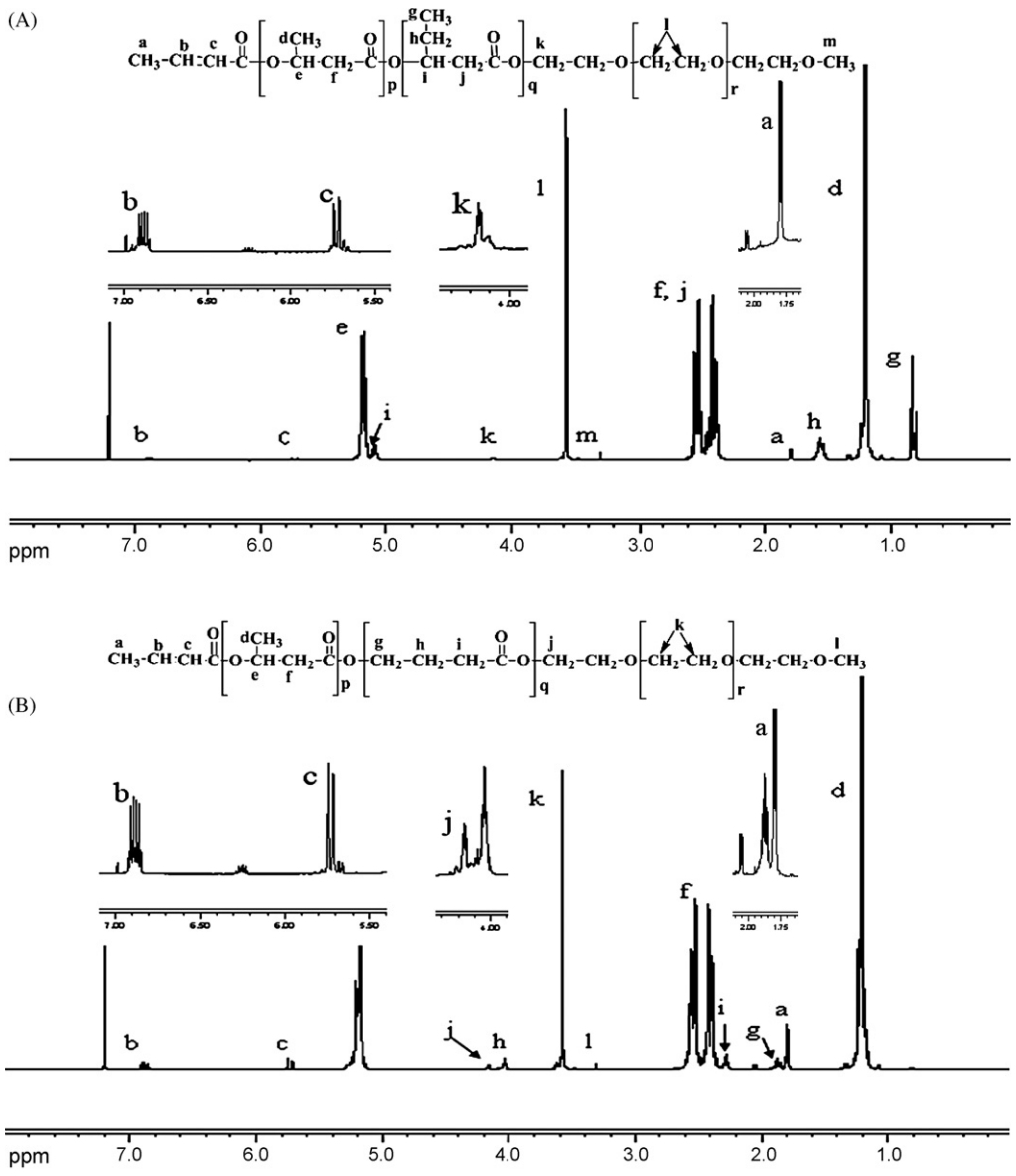

Fig. 3. ^{1}H NMR spectra of synthesized PHA–mPEG diblock copolymers: (A) P(3HB-*co*-12 mol% 3HV)–mPEG; (B) P(3HB-*co*-6 mol% 4HB)–mPEG.

effect on the surface barrier was found in the degradation of hydrocarbon (C12–C14) end-capped poly(L-lactide) film by proteinase K (Kurokawa et al., 2008). They suggested that the slower degradation, compared to non-end-capped polymer film, must be due to the coverage of the hydrocarbon end groups on the surface. Therefore, the slower degradation of PHA–mPEG nanoparticles clearly indicated that the amphiphilic nanoparticles form a concealed core of hydrophobic copolymer surrounded by the hydrophilic mPEG segment when suspended in aqueous solution. As far as we know, this enzymatic study is the first direct experimental evidence for the PHA-core and mPEG-shell topography in aqueous solution.

3.3. In vitro drug release

Most of the hydrophobic drugs when administered to the body are often precipitated and degraded in the blood stream without reaching the target zone, and thus cause severe side affects (Dutta et al., 2009). TQ, the major biologically active component isolated from a traditional medicinal herb, *Nigella sativa* Linn., is a potential chemopreventive and chemotherapeutic compound (El-Mahdy et al., 2005). The chemical structure of TQ is shown in Fig. 6A. TQ is commonly known as an anticancer agent and was also reported to show neuroprotective effects (Gali-Muhtasib et al., 2008; Kanter, 2008). Despite of its widespread therapeutic applications, TQ is

Table 2
Particle sizes, polydispersities, surface charges drug loading and encapsulation efficiency of the PHA–mPEG nanoparticles.

Diblock copolymer	Particle size (nm) ± SD	Polydispersity index ± SD	Zeta potential (mV) ± SD	Encapsulation efficiency (%)
P(3HB-*co*-12 mol% 3HV)–mPEG	162 ± 8	0.376 ± 0.003	−19 ± 3	43 ± 2
P(3HB-*co*-33 mol% 3HV)–mPEG	125 ± 2	0.296 ± 0.002	−18 ± 1	57 ± 3
P(3HB-*co*-6 mol% 4HB)–mPEG	119 ± 2	0.724 ± 0.003	−22 ± 1	29 ± 4
P(3HB-*co*-20 mol% 4HB)–mPEG	112 ± 3	0.218 ± 0.004	−27 ± 2	34 ± 2

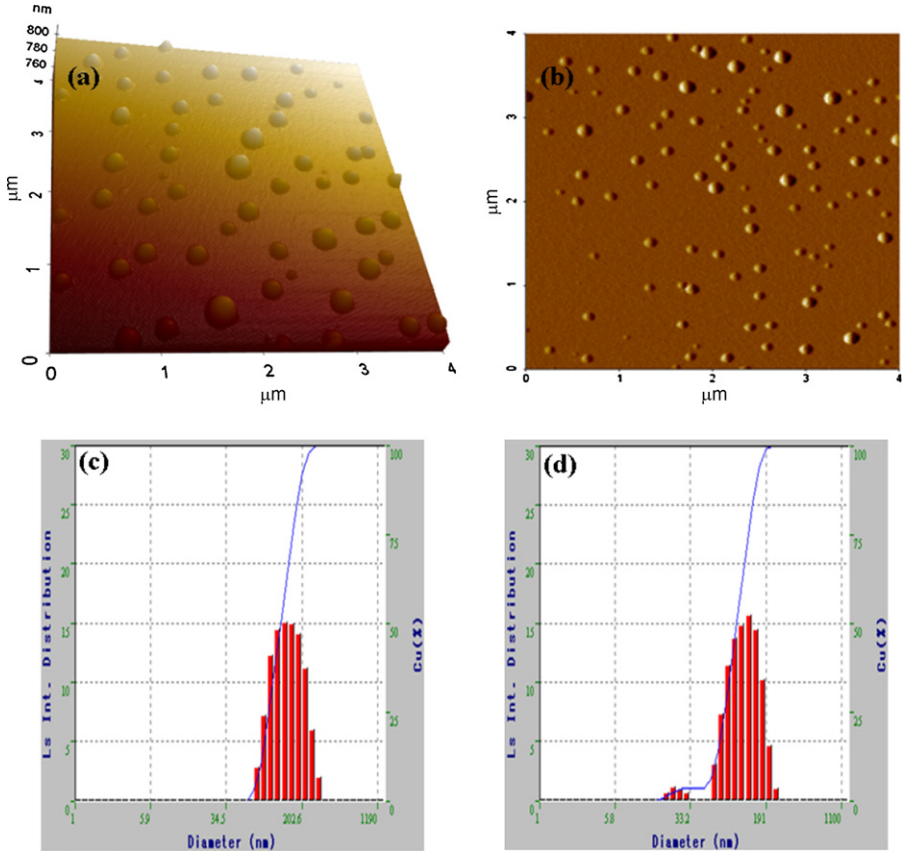

Fig. 4. Characterization of the PHA–mPEG nanoparticles. AFM images of the nanoparticles: (A) A 3-D AFM image of P(3HB-*co*-33 mol% 3HV)–mPEG nanoparticles with a scan size of 4 μm × 4 μm; (B) P(3HB-*co*-20 mol% 4HB)–mPEG nanoparticles with a scan size of 4 μm × 4 μm. Size distribution of the nanoparticles determined by DLS: (C) P(3HB-*co*-33 mol% 3HV)–mPEG nanoparticles; (D) P(3HB-*co*-20 mol% 4HB)–mPEG nanoparticles.

hydrophobic in nature and has poor water solubility that limits the dosage and usage of the drug in most of the clinical trials. In order to study the bioavailability and controlled release of TQ from PEGylated nanoparticles, the drug was encapsulated in the PHA–mPEG nanoparticles and its release kinetics was studied *in vitro*.

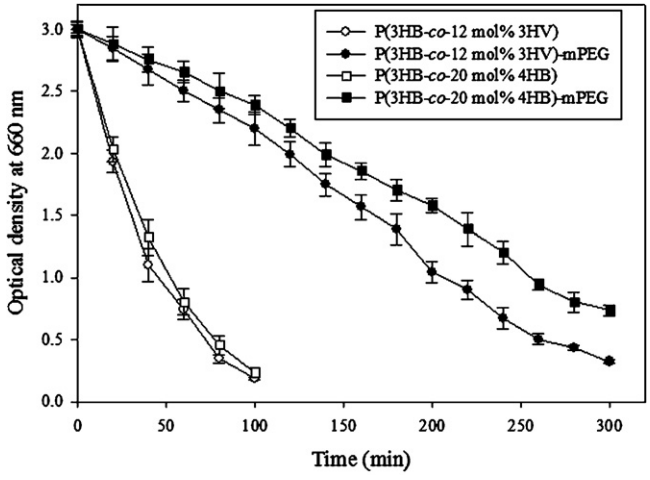

Fig. 5. Relative enzymatic degradation of copolymer nanoparticles to determine the localization of PHA and mPEG segment in nanoparticles: open symbols for controls – (○) P(3HB-*co*-12 mol% 3HV); (□) P(3HB-*co*-20 mol% 4HB) nanoparticles; closed symbols – (●) P(3HB-*co*-12 mol% 3HV)–mPEG; (■) P(3HB-*co*-20 mol% 4HB)–mPEG nanoparticles.

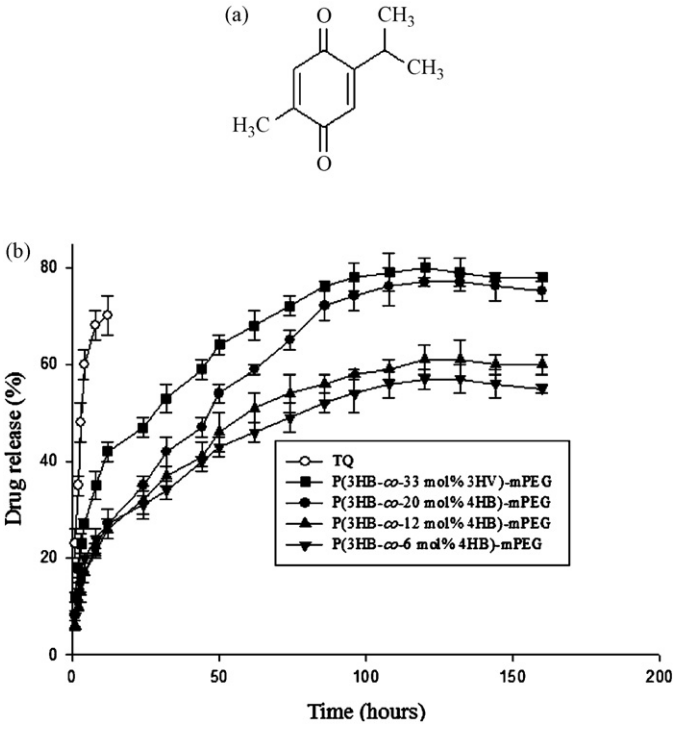

Fig. 6. *In vitro* release profiles of TQ encapsulated nanoparticles: (A) chemical structure of TQ; (B) release profiles of free TQ and TQ loaded PHA–mPEG nanoparticles.

Fig. 6B shows the *in vitro* release profiles of free TQ and TQ loaded PHA–mPEG nanoparticles in PBS at 37 °C. All the PEGylated nanoparticles showed similar release profiles of initial burst release of TQ from the nanoparticles followed by a sustained release. However, the release of TQ from P(3HB-*co*-33 mol% 3HV)–mPEG and P(3HB-*co*-20 mol% 4HB)–mPEG was little faster at the initial burst release phase compared to that of P(3HB-*co*-12 mol% 3HV) and P(3HB-*co*-6 mol% 4HB) nanoparticles. About 30–40% of the drug was released in the initial burst release phase from P(3HB-*co*-33 mol% 3HV)–mPEG and P(3HB-*co*-20 mol% 4HB)–mPEG nanoparticles. In the case of P(3HB-*co*-12 mol% 3HV) and P(3HB-*co*-6 mol% 4HB) nanoparticles the release was little slower at the initial stage of incubation and almost 20–30% of the encapsulated drug contributed to the initial burst release phase. In P(3HB-*co*-33 mol% 3HV)–mPEG and P(3HB-*co*-20 mol% 4HB)–mPEG nanoparticles the release of the drug reached its maximum limits at about 120 h with almost 70–80% release of the encapsulated drug. While in P(3HB-*co*-12 mol% 3HV)–mPEG and P(3HB-*co*-6 mol% 4HB) nanoparticles the sustained release was attained at 40–50 h and reached at its maximum limits at about 100 h with 50–60% loss of the drug. The relatively rapid release rate of the nanoparticles containing high amount of 3HV or 4HB comonomer units might be due to the higher encapsulation efficiency of the nanoparticles compared to that of low comonomer units in the composition (Table 2). A similar trend of higher encapsulation efficiency of TCN loaded microspheres with higher 3HV comonomer unit in the composition was observed by Sendil et al. (1999). The initial fast release of the drug from nanoparticles was suggested that some amount of the drug was absorbed on the surface or loosely bound to the inner polymer core and was lost during the initial stage of incubation (Allen et al., 1999), while the strongly encapsulated drug in the core domains followed slow and sustained release kinetics. The slow release of the drug from the core domains of the nanoparticles was attributed to the hydrophobic interactions between the hydrophobic drugs and hydrophobic polymer core (Liu et al., 2000). In contrast, almost 70% of the free TQ was released into the medium within 6–8 h showing the diffusional release of the drug from dialysis membrane (Fig. 6B). This result indicates that the PHA–mPEG nanoparticles effectively extended the release of TQ and can be used for the controlled delivery of hydrophobic drugs.

3.4. *In vitro* evaluation of biocompatibility

3.4.1. Cytotoxicity of the nanoparticles

The cytotoxic effect of amphiphilic nanoparticles was evaluated under *in vitro* conditions in prenatal rat neuronal hippocampal cells (Fig. 7A) and NIH/3T3 fibroblast cell line (Fig. 7B) by MTT assay using increasing doses of nanoparticles. In the MTT assay, the viable cells metabolize MTT dye to a water insoluble purple formazan product which can be analyzed spectrophotometrically. After incubation, the neuronal cells showed excellent viability even at concentrations up to 400 μg/mL of the nanoparticles (Fig. 7A). However, upon increasing the concentration of nanoparticles above 400 μg/mL a slight decrease in the viability of cells was observed. A little augmented toxicity compared to P(3HB-*co*-20 mol% 4HB)–mPEG nanoparticles was observed when the cells were incubated with P(3HB-*co*-33 mol% 3HV)–mPEG nanoparticles at the concentration of 500 μg/mL (Fig. 7A). Our findings are in agreement with those of cells incubated with higher concentration of P(3HB-*co*-4HB) polymer showing the biocompatibility of this polymer to the cells (Siew et al., 2007). A similar effect was observed when fibroblast cells were incubated with P(3HB-*co*-33 mol% 3HV)–mPEG and P(3HB-*co*-20 mol% 4HB)–mPEG nanoparticles (Fig. 7B). At low concentrations both of the nanoparticles showed little cytotoxic response. As the concentration of the PHA–mPEG nanoparticles

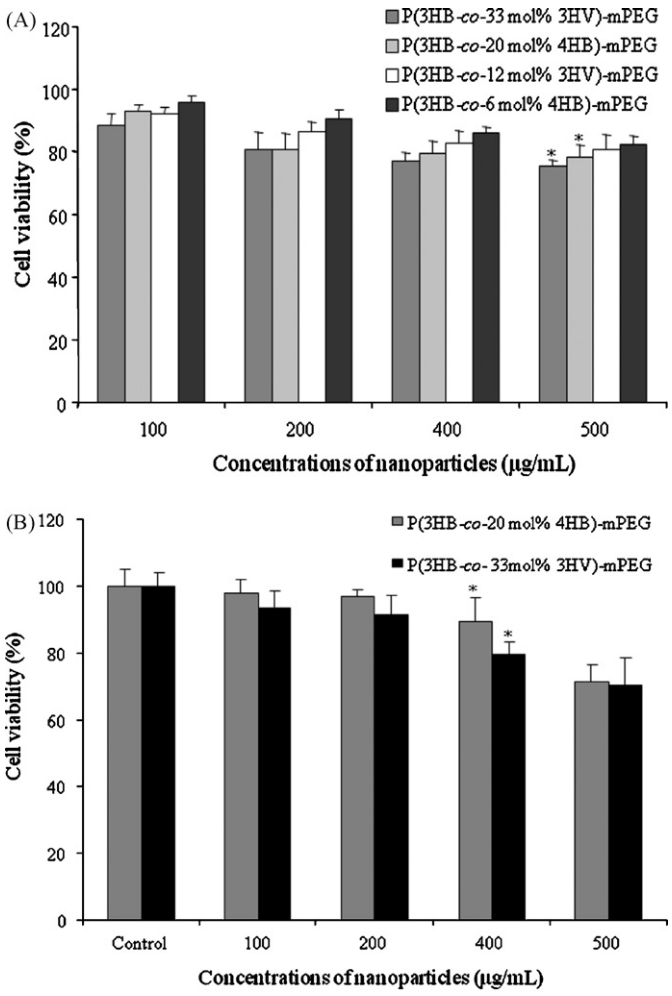

Fig. 7. Cytocompatibility evaluation of the prepared nanoparticles: (A) viability of primary neuronal cell culture incubated with four different types of copolymer nanoparticles; (B) viability of NIH/3T3 fibroblast cell culture with two different types of nanoparticles: cells were seeded in 96-well plates and incubated with desired concentrations (100–500 μg/mL) of the nanoparticles in DMEM for 24 h. Cell viability was measured by MTT assay. The viability of control cells was considered as 100%. Detail procedure is mentioned in Section 2. $^*P < 0.05$, based on repeated measures ANOVA (student's *t*-test). Data shown as mean ± SD ($n = 4$) with 4 plates in each experiment of the specific absorbance.

increased from 100 to 500 μg/mL in the culture medium, a slight decrease in the viability of the cells was observed. Similar to neuronal cell culture the cytotoxic effect was slightly higher for P(3HB-*co*-33 mol% 3HV)–mPEG nanoparticles as compared to P(3HB-*co*-20 mol% 4HB)–mPEG nanoparticles. However, both of the nanoparticles showed slightly increased cytotoxicity when the concentration of nanoparticles was increased (500 μg/mL). A little augmented toxicity observed in the case of P(3HB-*co*-33 mol% 3HV)–mPEG nanoparticles might be due to the activation of inflammatory responses most probably by the 3HV unit of the polymer (Gogolewski et al., 1993).

3.4.2. Neuronal cell death

We evaluated neuronal cell death for the assessment of effect of nanoparticles on the viability of cells. Neuronal cells were selected for the *in vitro* evaluation of biocompatibility of the nanoparticles because of the high sensitivity of these cells to foreign objects (Anderson, 2004). Neuronal cells were treated with different dilutions of nanoparticles for 24 h. FJB staining was used to identify degenerating neurons after survival periods as a reliable marker for neuronal vulnerability (Anderson et al., 2005). The cells were

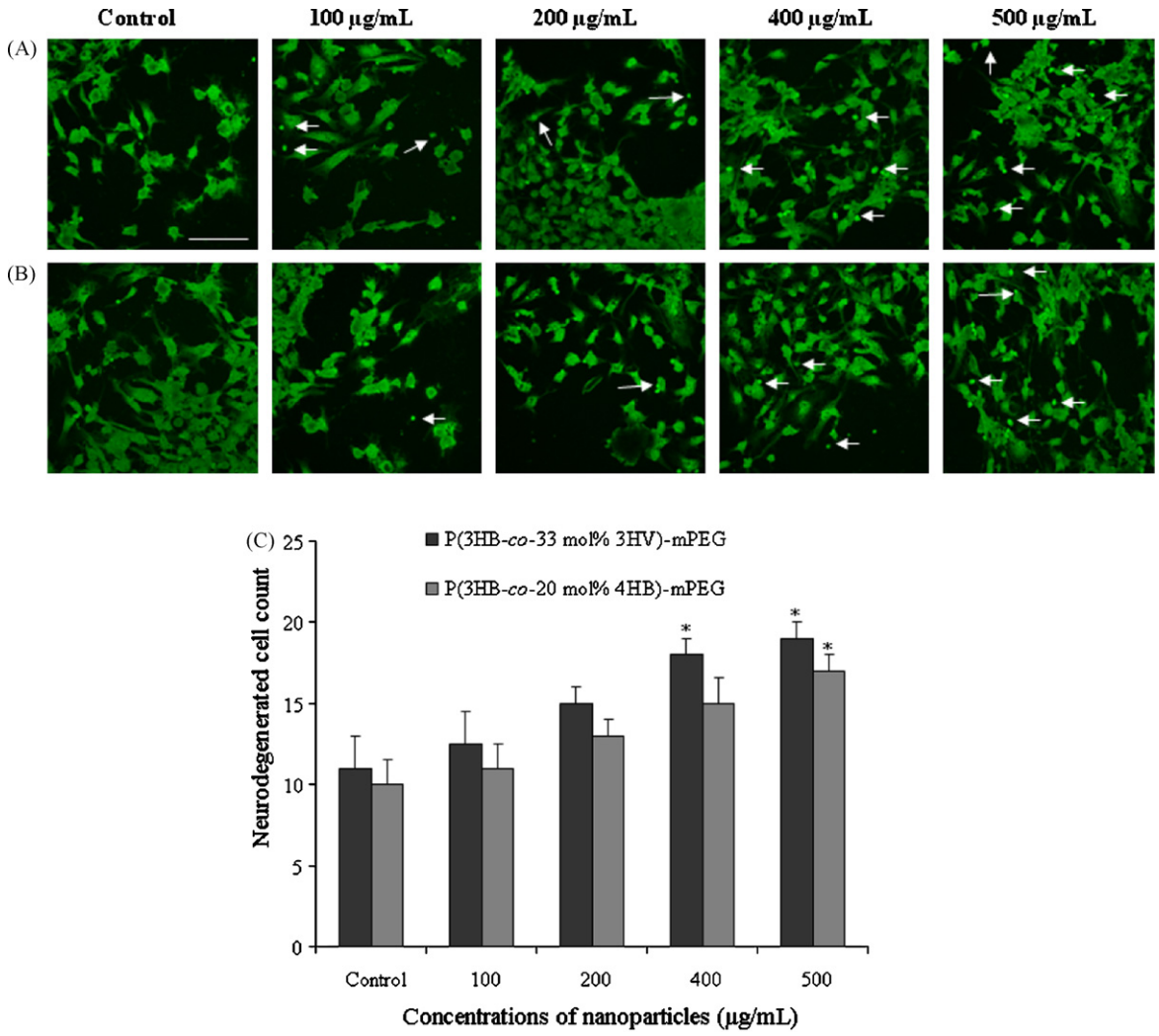

Fig. 8. The effect of polymeric nanoparticles on the structure of prenatal rat hippocampal neuronal cells and the induction of neurodegeneration. (A) P(3HB-*co*-33 mol% 3HV)–mPEG nanoparticles. (B) P(3HB-*co*-20 mol% 4HB)–mPEG nanoparticles. (C) Cell death was measured on 10 randomly selected fields in each slide ($n = 3$) at 400× magnification for P(3HB-*co*-33 mol% 3HV)–mPEG and P(3HB-*co*-20 mol% 4HB)–mPEG nanoparticles, respectively. The cells treated without nanoparticles were used as control. The percentage of cells death was measured by FJB staining as described in Section 2. Cells undergoing neurodegeneration are shown by arrows. $^{*}P < 0.05$. Scale bar: 20 μm.

labeled with FJB immuno-fluorescence staining and cellular death was observed as signal for the indication of apoptosis using confocal microscopy. As depicted in Fig. 8A and B, despite the relatively large dosage of the nanoparticles, no significant alterations in cells shape and distribution of cells number were detected relative to control cells. The cells treated with nanoparticles as stained with FJB (shown in green) in confocal microscope were well spread and the dendrites outgrowth in neuronal cells were increased and made connection with adjacent cells expressing full dendrites and neurofilaments. No significant changes in the expression of neurofilaments were observed and less numbers of dead cells were formed while treating the cells with low dilutions of the nanoparticles relative to control cells (dead cells shown by arrows). However, compared with P(3HB-*co*-20 mol% 4HB)–mPEG, the number of cells undergoing neuronal degeneration to that of total amount of cells were slightly increased with addition of high concentrations of P(3HB-*co*-33 mol% 3HV)–mPEG nanoparticles (Fig. 8A and B). This clearly indicates that increased amount of cell death might be due to the high amount of 3HV comonomer unit in the composition. In contrast, a reduced amount of cell death was observed when the cells were treated with either P(3HB-*co*-12 mol% 3HV)–mPEG and P(3HB-*co*-6 mol% 4HB)–mPEG nanoparticles (data not shown). The percentages of cells treated with P(3HB-*co*-33 mol% 3HV)–mPEG and P(3HB-*co*-20 mol% 4HB)–mPEG nanoparticles at different concentrations together with control cells are shown in Fig. 8C. The percentages of neurodegeneration in the cells treated with low amount of comonomer units of both 3HV and 4HB showed slight effect on cellular death (data not shown). These results clearly demonstrated that the mPEG provide a nontoxic coating on the surface of PHA copolymers. Introduction of mPEG on the surface of the copolymers greatly enhances the stability and amphiphilicity of the particles making them an easy source to assemble into nano-size core–shell structures in aqueous solution. The preparation of nanoparticles from such core–shell copolymers will enhance the safe delivery of variety of drugs.

4. Conclusions

In this study, the preparation of diblock copolymers was carried out by chemical combination of PHA copolymers and mPEG using bis(2-ethylhexanoate) tin as a transesterification catalyst. Characterization of the product was performed by GPC, ^{1}H NMR and DSC analysis. Enzymatic degradation analysis of the diblock copolymers suggested that the nanoparticles prepared from such

two phase system assembled into amphiphilic nanoparticles with inner concealed core of hydrophobic PHA copolymer and exposed shell of hydrophilic mPEG in aqueous solution. The average diameter of the nanoparticles was in the range of 100–200 nm with surface charge of −18 to −27 mV, respectively. The encapsulation and release kinetics for drug like TQ showed that the nanoparticles can be used as extended delivery nanocontainers for hydrophobic drugs. The *in vitro* cell viability studies indicated that the nanoparticles with core–shell structures show compatibility in biological environment. These results indicate that the nanoparticles prepared from PHA copolymers with mPEG surface modification could provide a safe and nontoxic system for the loading of drugs without producing any significant toxic effects on the cell survival and is presumed to be a promising vehicle for the administration of hydrophobic drugs.

Acknowledgments

This study was supported by a grant from the MEST/NRF to the Environmental Biotechnology National Core Research Center (grant #: 20090091 489). M.S. and M.I.N. were supported by a graduate scholarship through the Environmental Biotechnology National Core Research Center and BK21 program.

References

Allen, C., Maysinger, D., Eisenberg, A., 1999. Nano-engineering block copolymer aggregates for drug delivery. Colloids Surf. B: Biointerfaces 16, 3–27.

Anderson, A.J., Dawes, E.A., 1990. Occurrence, metabolism, metabolic role, and industrial uses of bacterial polyhydroxyalkanoates. Microbiol. Rev. 54, 450–472.

Anderson, J.K., 2004. Oxidative stress in neurodegeneration: cause or consequence? Nat. Rev. Neurosci. 5, S18–S25.

Anderson, K.J., Miller, K.M., Fugaccia, I., Scheff, S.W., 2005. Regional distribution of Fluoro-Jade B staining in the hippocampus following traumatic brain injury. Exp. Neurol. 193, 125–130.

Avgoustakis, K., Beletsi, A., Panagi, Z., Klepetsanis, P., Livaniou, E., Evangelatos, G., Ithakissios, D.S., 2003. Effect of copolymer composition on the physicochemical characteristics, in vitro stability, and biodegradation of PLGA–mPEG nanoparticles. Int. J. Pharm. 259, 115–127.

Basu, S., Harfouche, R., Soni, S., Chimote, G., Mashelkar, R.A., Sengupta, S., 2009. Nanoparticles-mediated targeting of MAPK signaling predisposes tumor to chemotherapy. PNAS 106, 7957–7961.

Bisht, S., Maitra, A., 2009. Dextran–doxorubicin/chitosan nanoparticles for solid tumor therapy. WIREs Nanomed. Nanobiotechnol. 1, 415–425.

Budhian, A., Siegel, S.J., Winey, K.I., 2007. Haloperidol-loaded PLGA nanoparticles: systematic study of particle size and drug content. Int. J. Pharm. 336, 367–375.

Chen, C., Yu, C.H., Cheng, Y.C., Yu-Peter, H.F., Cheung, M.K., 2006. Biodegradable nanoparticles of amphiphilic triblock copolymers based on poly(3-hydroxybutyrate) and poly(ethylene glycol) as drug carriers. Biomaterials 27, 4804–4814.

Choi, M.H., Yoon, S.C., 1994. Polyester biosynthesis characteristics of *Pseudomonas citronellolis* grown on various carbon sources, including 3-methyl-brached substrates. Appl. Environ. Microbiol. 60, 3245–3254.

Choi, M.H., Yoon, S.C., Lenz, R.W., 1999. Production of poly(3-hydroxybutyric acid-*co*-4-hydroxybutyric acid) and poly(4-hydroxybutyric acid) without subsequent degradation by *Hydrogenophaga pseudoflava*. Appl. Environ. Microbiol. 65, 1570–1577.

Duan, Y., Sun, X., Gong, T., Wang, Q., Zhang, Z., 2006. Preparation of DHAQ-loaded mPEG–PLGA–mPEG nanoparticles and evaluation of drug release behaviors *in vitro*/*in vivo*. J. Mater. Sci. Mater. Med. 17, 509–516.

Duncan, R., 2006. Polymer conjugates as anticancer nanomedicine. Nat. Rev. Cancer 6, 688–701.

Dutta, P., Shrivastava, S., Dey, J., 2009. Amphiphilic polymer nanoparticles: characterization and assessment as new drug carriers. Macromol. Biosci. 9, 1116–1126.

El-Mahdy, M.A., Zhu, Q., Wang, Q.E., Wani, G., Wani, A.A., 2005. Thymoquinone induces apoptosis through activation of caspase-8 and mitochondrial events in p-53 null myeloblastic leukemia HL-60 cells. Int. J. Cancer 117, 409–417.

Fishburn, C.S., 2008. The pharmacology of PEGylation: balancing PD with PK to generate novel therapeutics. J. Pharm. Sci. 97, 4167–4183.

Gali-Muhtasib, H., Ocker, M., Kuester, D., Krueger, S., El-Hajj, Z., Diestel, A., Evert, M., El-Najjar, N., Peters, B., Jurjus, A., Roessner, A., Schneider-Stock, R., 2008. Thymoquinone reduces mouse colon tumor cell invasion and inhibits tumor growth in murine colon cancer models. J. Cell. Mol. Med. 12, 330–342.

Gaucher, G., Dufresne, M.H., Sant, V.P., Kang, N., Maysinger, D., Leroux, J.C., 2005. Block copolymer micelles: preparation, characterization and application in drug delivery. J. Control. Release 109, 169–188.

Gogolewski, S., Jovanovic, M., Perren, S.M., Dillon, J.G., Hughes, M.K., 1993. Tissue response and *in vivo* degradation of selected polyhydroxyacids: polylactides (PLA), poly(3-hydroxybutyrate) (PHB), and poly(3-hydroxybutyrate-*co*-3-hydroxyvalerate) (PHB/VA). J. Biomed. Mater. Res. A 27, 1135–1148.

Gref, R., Minamitake, Y., Peracchia, M.T., Trubetskoy, V., Torchilin, V., Langer, R., 1994. Biodegradable long-circulating polymeric nanospheres. Science 263, 1600–1603.

Hans, M.L., Lowman, A.M., 2002. Biodegradable nanoparticles for drug delivery and targeting. Curr. Opin. Solid State Mater. Sci. 6, 319–327.

Iwata, T., Doi, Y., Nakayama, S., Sasatsuki, H., Teramachi, S., 1999. Structure and enzymatic degradation of poly(3-hydroxybutyrate) copolymer single crystals with an extracellular PHB depolymerase from *Alcaligenes faecalis* T1. Int. J. Biol. Macromol. 25, 169–176.

Iyer, A.K., Khaled, G., Fang, J., Maeda, H., 2006. Exploiting the enhanced permeability and retention effect for tumor targeting. Drug Discov. Today 11, 812–818.

Jeong, I., Kim, B.S., Lee, H., Lee, K.M., Shim, I., Kang, S.K., Yin, C.S., Hahm, D.H., 2009. Prolonged analgesic effect of PLGA-encapsulated bee venom on formalin-induced pain in rats. Int. J. Pharm. 380, 62–66.

Johnson, J.E., 1995. Methods for cell death and viability in primary neuronal cultures. Methods Cell Biol. 46, 243–276.

Kanter, M., 2008. *Nigella sativa* and derived thymoquinone prevents hippocampal neurodegeneration after chronic toluene exposure in rats. Neurochem. Res. 33, 579–588.

Khang, G., Choi, H.S., Rhee, J.M., Yoon, S.C., Cho, J.C., Lee, H.B., 2000. Controlled release of gentamicin sulfate from poly(3-hydroxybutyrate-*co*-3-hydroxyvalerate) wafers for the treatment of osteomyelitis. Korean Polym. J. 8, 253–260.

Khang, G., Kim, S.W., Cho, J.C., Rhee, J.M., Yoon, S.C., Lee, H.B., 2001. Preparation and characterization of poly(3-hydroxybutyrate-*co*-3-hydroxyvalerate) microspheres for the sustained release of 5-fluorouracil. Bio-Med. Mater. Eng. 11, 89–103.

Köse, G.T., Ber, S., Korkusuz, F., Hasirci, V., 2003. Poly(3-hydroxybutyric acid-*co*-3-hydroxyvaleric acid) based tissue engineering matrices. J. Mater. Sci. Mater. Med. 14, 121–126.

Kumar, V., Homme, R.K.P., 2008. Thermodynamic limits on drug loading in nanoparticle cores. J. Pharm. Sci. 97, 4904–4914.

Kurokawa, K., Yamashita, K., Doi, Y., Abe, H., 2008. Structural effects of terminal groups on nonenzymatic and enzymatic degradations of end-capped poly(L-lactide). Biomacromolecules 9, 1071–1078.

Lenz, R.W., Marchessault, R.H., 2005. Bacterial polyesters: biosynthesis, biodegradable plastics and biotechnology. Biomacromolecules 6, 1–8.

Letchford, K., Burt, H., 2007. A review of the formation and classification of amphiphilic block copolymer nanoparticulate structures: micelles, nanospheres, nanocapsules and polymersomes. Eur. J. Pharm. Biopharm. 65, 259–269.

Lionzo, M.I.Z., Re, M.I., Guterres, S.S., Pohlmann, A.R., 2007. Microparticles prepared with poly(hydroxybutyrate-*co*-hydroxyvalerate) and poly(ε-caprolactone) blends to control the release of a drug model. J. Microencapsul. 24, 175–186.

Liu, M., Kono, K., Fréchet, J.M.J., 2000. Water-soluble dendritic unimolecular micelle: their potential as drug delivery agents. J. Control. Release 65, 121–131.

Maeda, H., Wu, J., Sawa, T., Matsumura, Y., Hori, K., 2000. Tumor vascular permeability and the EPR effect in macromolecular therapeutics: a review. J. Control. Release 65, 271–284.

Moghimi, S.M., Hunter, A.C., Murray, J.C., 2001. Long-circulating and target specific nanoparticles: theory to practice. Pharmacol. Rev. 53, 283–318.

Moghimi, S.M., Hedeman, H., Muir, I.S., Illum, L., Davis, S.S., 1993. An investigation of the filtration capacity and the fate of large filtered sterically stabilized microspheres in rat spleen. Biochim. Biophys. Acta 1157, 233–240.

Mosqueira, V.C.F., Legrand, P., Gulik, A., Bourdon, O., Gref, R., Labarre, D., Barratt, G., 2001. Relationship between complement activation, cellular uptake and surface physicochemical aspects of novel PEG-modified nanocapsules. Biomaterials 22, 2967–2979.

Naguyen, S., Yu, G., Marchessault, R.H., 2002. Thermal degradation of poly(3-hydroxyalkanoates): preparation of well-defined oligomers. Biomacromolecules 3, 219–224.

Naseer, M.I., Lee, H.Y., Kim, M.O., 2010. Neuroprotective effect of vitamin C against the ethanol and nicotine modulation of $GABA_B$ receptor and PK-α expression in prenatal rat brain. Synapse 64, 467–477.

Panyam, J., Labhasetwar, V., 2003. Biodegradable nanoparticles for drug and gene delivery to cells and tissue. Adv. Drug Deliv. Rev. 55, 329–347.

Pötter, M., Steinbüchel, A., 2005. Poly(3-hydroxybutyrate) granule-associated proteins: impacts on poly(3-hydroxybutyrate) synthesis and degradation. Biomacromolecules 6, 552–560.

Prabaharan, M., Grailer, J.J., Pilla, S., Steeber, D.A., Gong, S., 2009. Amphiphilic multi-arm block copolymer based on hyperbranched polyester, poly(L-lactide) and poly(ethylene glycol) as a drug delivery carrier. Macromol. Biosci. 9, 515–524.

Qu, X.H., Wu, Q., Zhang, K.Y., Chen, G.Q., 2006. *In vivo* studies of poly(3-hydroxybutyrate-*co*-3-hydroxyhexanoate) based polymers: biodegradation and tissue reactions. Biomaterials 27, 3540–3548.

Ravenelle, F., Marchessault, R.H., 2002. One-step synthesis of amphiphilic diblock copolymers from bacterial poly([R]-3hydroxybutyric acid). Biomacromolecules 3, 1057–1064.

Ravenelle, F., Marchessault, R.H., 2003. Self-assembly of poly([R]-3-hydroxybutyric acid-block-polyethylene glycol) diblock copolymers. Biomacromolecules 4, 856–858.

Ravindran, J., Nair, H.B., Sung, B., Prasad, S., Tekmal, R.R., Aggarwal, B.B., 2010. Thymoquinone poly(lactide-co-glycolide) nanoparticles exhibit enhanced anti-proliferative, anti-inflammatory, and chemosensitization potential. Biochem. Pharmacol. 79, 1640–1647.

Sendil, D., Gürsel, I., Wise, D.L., Hasirci, V., 1999. Antibiotic release from biodegradable PHBV microparticles. J. Control. Release 59, 207–217.

Shirakura, Y., Fukui, T., Saito, T., Okamoto, Y., Narikawa, T., Koide, K., Tomita, K., Takemasa, T., Masamune, S., 1986. Degradation of poly(3-hydroxybutyrate) depolymerase from *A. faecalis* T1. Biochim. Biophys. Acta 880, 46–53.

Siew, E.L., Rajab, N.F., Osman, A.B., Sudesh, K., Hussain, S.H.I., 2007. *In vitro* biocompatibility evaluation of poly(3-hydroxybutyrate-*co*-4-hydroxybutyrate) copolymers in fibroblast cells. J. Biomed. Mater. Res. A 81, 317–325.

Soppimath, K.S., Aminabhavi, T.M., Kulkarni, A.R., Rudzinski, W.E., 2001. Biodegradable polymeric nanoparticles as drug delivery devices. J. Control. Release 70, 1–20.

Tang, Y., Sing, J., 2009. Biodegradable and biocompatible thermosensitive polymers based injectable implant for controlled release of protein. Int. J. Pharm. 365, 34–43.

Timbart, L., Renard, E., Langlois, V., Guerin, P., 2004. Novel biodegradable copolyesters containing blocks of poly(3-hydroxyoctanoate) and poly(ε-caprolactone): synthesis and characterization. Macromol. Biosci. 4, 1014–1020.

Yao, Y.C., Zhan, X.Y., Zhang, J., Zou, X.H., Wang, Z.H., Xiong, Y.C., Chen, J., Chen, G.Q., 2008. A specific drug targeting system based on polyhydroxyalkanoate granule binding protein PhaP fused with targeted cell ligands. Biomaterials 29, 4823–4830.